Samuel Forest*

Questioning size effects as predicted by strain gradient plasticity

Abstract: The analytical solution of the elastic-plastic response of a two-phase laminate microstructure subjected to periodic simple shear loading conditions is derived considering strain gradient and micromorphic plasticity models successively. One phase remains purely elastic, whereas the second one displays an isotropic elastic-plastic behavior. Although no classic hardening is introduced at the individual phase level, the laminate is shown to exhibit an overall linear hardening scaling with the inverse of the square of the cell size. The micromorphic model leads to a saturation of the hardening at small length scales in contrast to Aifantis strain gradient plasticity model displaying unlimited hardening. The models deliver qualitatively relevant size effects from the physical metallurgical point of view, but fundamental quantitative discrepancy is pointed out and discussed, thus requiring the development of more realistic nonlinear equations in strain gradient plasticity.

***Corresponding author: Samuel Forest,** MINES ParisTech, Centre des matériaux, CNRS UMR 7633, BP 87, 91003 Evry cedex, France, Phone: +33-1-60-76-30-51, Fax: +33-1-60-76-31-50, e-mail: samuel.forest@ensmp.fr

1 Introduction

Strain gradient plasticity still is a promising extension of classic continuum mechanics to address size effects in the materials behavior. Although much progress has been gained in the continuum thermodynamics and mechanics formulations and the computational analysis of such models in the past 20 years, much remains to be done to formulate reliable constitutive equations that are able to account for the scaling laws observed in the mechanical responses of materials [1]. Examples of such scaling laws for metals and alloys are the Orowan $1/l$ relationship, linking the overall yield stress to precipitate size or spacing l, and the Hall-Petch $1/\sqrt{l}$ scaling, where l is the grain size.

Most implemented strain gradient plasticity models have been shown to deliver a size-dependent hardening response over a small range of grain sizes in the case of polycrystals for instance. The hardening behavior of polycrystals according to now well-established generalized crystal plasticity models has been shown in [2–5] to be strongly grain size dependent, but the scaling laws are either not provided or do not correspond to a Hall-Petch behavior reference. In addition to that, the strain gradient plasticity-induced extrahardening often displays a linear character that is too simplistic compared with realistic materials responses.

The objective of this work is to provide an analytical solution of a simple strain gradient plasticity boundary value problem that clearly shows the scaling between yield stress, work-hardening modulus, and the microstructure's characteristic length. The obtained scaling law will be compared with existing rules coming from the physical metallurgy. To make the example as simple as possible, Aifantis isotropic strain gradient plasticity model is used, instead of more elaborate single crystal models more directly related to the physics of deformation and for which such analytical results have already been derived in [6]. The presented solution will be shown to share several common features with the single crystal problem.

The considered physical situation is that of a two-phase laminate microstructure made of alternating layers of a purely elastic material and a plastically flowing material. Two generalized continuum approaches are compared: Aifantis original model incorporating the effect of the gradient of the cumulative plastic strain and a more recent micromorphic model including an additional plastic microdeformation variable. The theoretical relationships between both classes of models have been examined in [7, 8].

A discussion follows the presentation of the analytical results to question the relevance of the obtained scaling laws and to trigger incentives for the improvement of the constitutive equations of strain gradient plasticity models.

The following notations are used: $\boldsymbol{a}, \underline{\boldsymbol{a}}, \underline{\underline{\boldsymbol{a}}}, \underline{\underline{\underline{\boldsymbol{a}}}}$ denote tensors of rank 0, 1, 2, and 4, respectively. The gradient operator is denoted by $\boldsymbol{\nabla}$.

2 Thermomechanical formulation of strain gradient plasticity

The thermodynamics of local action is applicable to gradient models meaning that the constitutive behavior can be formulated by means of two potential functions of a set of independent state variables, namely, the free energy density function and a dissipation potential. This method is illustrated first for a simple isotropic micromorphic model and then specialized to Aifantis strain gradient plasticity, following [8].

The micromorphic theory has been proposed simultaneously by Eringen and Mindlin [9, 10]. It consists of introducing a general noncompatible field of microdeformation, in addition to the usual material deformation gradient, accounting for the deformation of a triad of microstructural directions. The micromorphic approach can, in fact, be applied to any macroscopic quantity to introduce an intrinsic length scale in the original standard continuum model in a systematic way, as done in [7].

As usual, the total strain is split into its elastic and plastic parts:

$$\underset{\sim}{\varepsilon}=\underset{\sim}{\varepsilon}^e+\underset{\sim}{\varepsilon}^p \tag{1}$$

According to the micromorphic approach, a microstrain variable p_χ is associated to p and regarded as an additional degree of freedom. The material behavior is then assumed to depend on the micromorphic variable and its gradient. Accordingly, the sets of degrees of freedom and the state space are enhanced as follows:

$$DOF=\{\underline{\boldsymbol{u}},p_\chi\},\ STATE=\{\underset{\sim}{\varepsilon}^e,p,\alpha,p_\chi,\nabla p_\chi\} \tag{2}$$

The principle of virtual power is generalized to incorporate the microstructural effects. This represents a systematic use of the method of virtual power that Germain applied to Eringen's micromorphic medium [11]. The classic power densities of internal and contact forces are extended in the following way:

$$p^{(i)}=\underset{\sim}{\boldsymbol{\sigma}}:\dot{\underset{\sim}{\varepsilon}}+a\dot{p}_\chi+\underline{\boldsymbol{b}}\cdot\nabla\dot{p}_\chi,\ p^{(c)}=\underline{\boldsymbol{t}}\cdot\underline{\dot{\boldsymbol{u}}}+a^c\dot{p}_\chi \tag{3}$$

in which generalized stresses a and $\underline{b}$ have been introduced. The application of the method of virtual power leads to the following additional local balance equation and boundary conditions, in addition to the classic local balance of momentum and traction conditions at the outer boundary:

$$\mathrm{div}\,\underline{\boldsymbol{b}}-a=0,\quad \forall\underline{\boldsymbol{x}}\in\Omega,\quad a^c=\underline{\boldsymbol{b}}\cdot\underline{\boldsymbol{n}},\quad \forall\underline{\boldsymbol{x}}\in\partial\Omega \tag{4}$$

The microstructural effects therefore arise in the balance of energy in the form:

$$\rho\dot{\epsilon}=p^{(i)}-\mathrm{div}\,\underline{\boldsymbol{q}}+\rho r \tag{5}$$

where ϵ is the specific internal energy, $\underline{\boldsymbol{q}}$ is the heat flux vector, and r is the external heat sources. The free energy density function ψ is assumed to be a function of the previous set *STATE*. The entropy principle is formulated in the form of the Clausius-Duhem inequality

$$-\rho\dot{\psi}+p^{(i)}\geq 0 \tag{6}$$

in the isothermal case for simplicity. In this work, the following state laws are postulated:

$$\underset{\sim}{\boldsymbol{\sigma}}=\rho\frac{\partial\psi}{\partial\underset{\sim}{\varepsilon}^e},\quad a=\rho\frac{\partial\psi}{\partial p_\chi},\quad \underline{\boldsymbol{b}}=\rho\frac{\partial\psi}{\partial\nabla p_\chi},\quad R=\rho\frac{\partial\psi}{\partial p},\quad X=\rho\frac{\partial\psi}{\partial\alpha} \tag{7}$$

State equations relate the generalized stresses to the microstrain variable and its gradient, assuming, for simplicity, that no dissipation is associated with them. This restriction will be sufficient to recover the targeted class of models. The thermodynamic forces associated with internal variables are R and X. The residual dissipation therefore is

$$D^{res}=\underset{\sim}{\boldsymbol{\sigma}}:\dot{\underset{\sim}{\varepsilon}}^p-R\dot{p}-X\dot{\alpha}\geq 0 \tag{8}$$

as in the classic case. The plastic behavior is characterized by the yield function $f(\underset{\sim}{\boldsymbol{\sigma}},R,X)$. In the micromorphic model, the yield function can still be treated as the dissipation potential providing the flow and evolution rules for internal variables. This corresponds to the hypothesis of maximal dissipation:

$$\dot{\underset{\sim}{\varepsilon}}^p=\dot{\lambda}\frac{\partial f}{\partial\underset{\sim}{\boldsymbol{\sigma}}},\quad \dot{p}=-\dot{\lambda}\frac{\partial f}{\partial R},\quad \dot{\alpha}=-\dot{\lambda}\frac{\partial f}{\partial X} \tag{9}$$

where $\dot{\lambda}$ is the plastic multiplier. At this stage, a coupling between the macroscopic and microscopic variables must be introduced, for instance, via the relative cumulative plastic strain p-p_χ.

A quadratic form is now proposed for the free energy density function, with respect to elastic strain, cumulative plastic strain, relative plastic strain, and micromorphic plastic strain gradient:

$$\rho\psi(\underset{\sim}{\varepsilon}^e,p,p_\chi,\nabla p_\chi)=\frac{1}{2}\underset{\sim}{\varepsilon}^e:\underset{\sim}{\boldsymbol{C}}:\underset{\sim}{\varepsilon}^e+\frac{1}{2}Hp^2+\frac{1}{2}H_\chi(p-p_\chi)^2+\frac{1}{2}A\nabla p_\chi.\nabla p_\chi \tag{10}$$

The corresponding classic model describes an elastoplastic material behavior with linear elasticity characterized by the tensor of elastic moduli $\underset{\sim}{\underset{\sim}{\boldsymbol{C}}}$ and the linear hardening modulus H. Isotropy has been assumed for the last term for the sake of brevity. Two additional material parameters are introduced in the micromorphic extension of this classic model, namely, the coupling modulus H_χ (MPa) and the micromorphic stiffness A (MPa mm^2). The thermodynamic forces associated with the state variables are given by the relations (7):

$$\underset{\sim}{\boldsymbol{\sigma}}=\underset{\sim}{\underset{\sim}{\boldsymbol{C}}}:\underset{\sim}{\varepsilon}^e,\quad a=-H_\chi(p-p_\chi),\quad \underline{\boldsymbol{b}}=A\nabla p_\chi,\quad R=(H+H_\chi)p-H_\chi p_\chi \tag{11}$$

Note that when the relative plastic strain $e=p-p_\chi$ is close to zero, the linear hardening rule retrieves its classic form and the generalized stress a vanishes. Only the strain gradient effect ∇p remains in the enriched work of internal forces (3). This is the situation encountered in the strain gradient plasticity models developed in [12]. When inserted in the additional balance equation (4), the previous state laws lead to the following partial differential equation:

$$p_\chi-\frac{A}{H_\chi}\Delta p_\chi=p \tag{12}$$

which is identical to the additional partial differential equation used in the so-called implicit gradient-enhanced elastoplasticity in [13]. The microstrain p_χ is called there the "nonlocal strain measure" $\overline{p}$. Note, however, that the latter model involves only one additional material parameter, namely, $l_c^2=A/H_\chi$, instead of two in the micromorphic approach.

In the micromorphic approach, the coupling modulus H_χ plays a central role and makes it possible to have a fully consistent thermomechanical basis for the model. When its value is high enough, it acts as a penalty term forcing the micromorphic plastic strain to follow the macroscopic one as close as possible.

The necessity of an additional boundary condition associated with the nonlocal strain measure has already been recognized in [13]. The associated Neumann condition is used in the form:

$$\nabla p_\chi.\underline{\boldsymbol{n}}=0\quad\text{on}\quad\partial\Omega \tag{13}$$

It coincides with the more general boundary condition derived from the micromorphic approach:

$$\underline{\boldsymbol{b}}\cdot\underline{\boldsymbol{n}}=a^c\quad\text{on}\quad\partial\Omega \tag{14}$$

when $a^c=0$ and when $\underline{\boldsymbol{b}}$ depends linearly on ∇p_χ, as it is the case for the quadratic potential (10).

The yield function is now chosen as

$$f(\underset{\sim}{\boldsymbol{\sigma}},R)=\sigma_{eq}-\sigma_Y-R \tag{15}$$

where σ_{eq} is an equivalent stress measure and σ_Y is the initial yield stress. The hardening rule then takes the following form:

$$R=\rho\frac{\partial\psi}{\partial p}=(H+H_\chi)p-H_\chi p_\chi \tag{16}$$

After substituting the balance equation (12) into the hardening law, yielding takes place when

$$\sigma_{eq}=\sigma_Y+Hp_\chi-A\left(1+\frac{H}{H_\chi}\right)\Delta p_\chi \tag{17}$$

This expression coincides with the enhanced yield criterion originally proposed for gradient plasticity in [14–16] and used for strain localization simulations in [17–19] when the micromorphic variable remains as close as possible to the plastic strain: $p_\chi\simeq p$. In the original work, the Laplace operator is directly introduced in the yield function either as a postulate or as a consequence of dislocation flux in the elementary volume, whereas its presence is derived here from the combination of the additional balance equation and the linear generalized constitutive equations.

As a result, Aifantis' model has been retrieved from the micromorphic approach by choosing simple linear constitutive equations and introducing the internal constraint $p_\chi\equiv p$, stating that the micromorphic variable coincides with the plastic strain itself. The original Aifantis model can also be directly constructed through a gradient type of internal variable model, as already done by several authors [16, 20, 21]. In particular, a recent contribution [22] rests upon the energy storage due to gradient of plastic strain to derive this class of models in the same way as in [16]. More general dissipative mechanisms can also be added.

3 Size effect in a laminate according to isotropic strain gradient plasticity

Laminate microstructures are prone to size effects, especially in the case of metals for which the interfaces act

as barriers for the dislocations. The material response then strongly depends on the layer thickness. This situation has been considered for Cosserat and micromorphic single crystals under single and double slip in [6, 23, 24]. The laminate microstructure is considered here in the case of Aifantis isotropic model. It is a periodic arrangement of two phases including a purely elastic material and a plastic strain gradient layer. The unit cell corresponding to this arrangement is shown in Figure 1. It is periodic along all three directions of the space. It must be replicated in the three directions to obtain the complete multilayer material. The thickness of the hard elastic layer is h, whereas the thickness of the soft plastic strain gradient layer is s.

The unit cell size is $l=s+h$ and the soft phase volume fraction is $f=s/l$.

Both phases are assumed to share the same elastic properties for simplicity. More general results, but without fundamental difference, may be derived from [6].

3.1 Position of the problem

The unit cell of Figure 1 is subjected to a mean simple shear $\overline{\gamma}$ in direction 1. The origin O of the coordinate system is the center of the soft phase. The displacement field is of the form

$$u_1=\overline{\gamma}\,x_2,\ u_2(x_1)=u(x_1),\ u_3=0 \tag{18}$$

where $u(x_1)$ is a periodic function that describes the fluctuation from the homogeneous shear. This fluctuation is the main unknown of the boundary value problem. The gradient of the displacement field and strain tensors are computed as follows:

$$[\nabla\underline{\boldsymbol{u}}]=\begin{bmatrix}0 & \overline{\gamma} & 0\\ u_{,1} & 0 & 0\\ 0 & 0 & 0\end{bmatrix},\quad [\underset{\sim}{\varepsilon}]=\begin{bmatrix}0 & \frac{1}{2}(\overline{\gamma}+u_{,1}) & 0\\ \frac{1}{2}(\overline{\gamma}+u_{,1}) & 0 & 0\\ 0 & 0 & 0\end{bmatrix} \tag{19}$$

where $u_{,1}$ denotes the derivative of the displacement u with respect to x_1. After Hooke's law, the only activated simple stress component is σ_{12}. Due to the balance of momentum equation and the continuity of the traction vector, this stress component is homogeneous throughout the laminate.

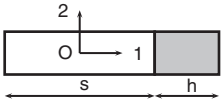

Figure 1 Unit cell of a periodic two-phase laminate.

The plastic flow rule takes the usual form for a von Mises material:

$$\underset{\sim}{\dot{\boldsymbol{\varepsilon}}}^p=\frac{3}{2}\dot{p}\frac{\underline{\boldsymbol{s}}}{J_2(\underline{\boldsymbol{\sigma}})},\quad \underset{\sim}{\dot{\boldsymbol{\varepsilon}}}^p=\frac{\sqrt{3}}{2}\dot{p}(\underline{\boldsymbol{e}}_1\otimes\underline{\boldsymbol{e}}_2+\underline{\boldsymbol{e}}_2\otimes\underline{\boldsymbol{e}}_1) \tag{20}$$

where $\underline{\boldsymbol{s}}$ is the deviatoric part of the stress tensor and $J_2(\underline{\boldsymbol{\sigma}})$ is the von Mises equivalent stress, equal to $\sqrt{3}|\sigma_{12}|$ in the present case. The cumulative plastic strain variable is p, with $\dot{p}$ being the plastic multiplier.

The elastic law in the elastic phase and the elastic-plastic response of the soft phase are then exploited in the next section to derive the partial differential equations for plastic strain and, finally, for the displacement fluctuation. The explicit solution is found after considering precise interface conditions regarding continuity of various variables.

Note that the solution is known for conventional plasticity, that is, in the absence of strain gradient effect. The plastic strain is expected to be homogeneous in the soft phase for any loading $\overline{\gamma}$. Plastic strain therefore exhibits the usual jump at the interface. The introduction of higher-order interface conditions, associated with strain gradient plasticity, will induce a nonhomogeneous plasticity field.

The solution was given in [25] in the case of a linear hardening soft phase. The size-dependent response of the laminate is analyzed below in the absence of classic hardening.

3.2 Detailed solution

Stress equilibrium requires σ_{12} to be uniform throughout the laminate at each loading step. In the elastic zone, the stress is given by

$$\sigma_{12}=\mu(\overline{\gamma}+u^h_{,1})\ \Rightarrow\ u^h_{,1}=C,\quad u^h=Cx_1+D \tag{21}$$

where the integration constants are in red color.

In the soft phase, the von Mises yield condition is assumed to be fulfilled:

$$\sqrt{3}\sigma_{12}=R_0-cp_{,11} \tag{22}$$

where $c[=A$ from (17)] is a material parameter. Note that linear hardening is excluded in the soft phase to more

clearly exhibit the strain gradient effect, meaning that $H=0$ in (10). Space differentiation of the previous equation implies that the plastic strain profile is parabolic:

$$p=\alpha\left(x_1^2-\frac{s^2}{4}\right) \tag{23}$$

where the parity of the function was taken into account. Also, the condition that p be continuous at the interface $x_1=\pm s/2$, meaning that $p(\pm s/2)=0$ has been enforced.

The displacement in the soft phase is derived from the elasticity law in the form:

$$\begin{aligned}&\sigma_{12}=\mu(\bar{\gamma}+u^s_{,1}-\sqrt{3}p) \quad\Rightarrow\quad u^s_{,1}=C+\sqrt{3}p,\\ &u^s=\left(C-\alpha\sqrt{3}\frac{s^2}{4}\right)x_1+\alpha\frac{\sqrt{3}}{3}x_1^3\end{aligned} \tag{24}$$

The rigid body translation has been chosen such that $u^s(0)=0$. The three integration constants arising in the previous equations are identified by means of the three following interface conditions:

– Displacement continuity at $x_1=\pm s/2$

$$u^s\left(\frac{s}{2}\right)=u^h\left(\frac{s}{2}\right) \quad\Rightarrow\quad -\sqrt{3}\alpha\frac{s^3}{12}=D \tag{25}$$

– Displacement periodicity at $x_1=-s/2$ and $x_1=s/2+h$

$$u^s\left(-\frac{s}{2}\right)=u^h\left(\frac{s}{2}+h\right) \quad\Rightarrow\quad \sqrt{3}\alpha\frac{s^3}{12}=Cl+D \tag{26}$$

– Continuity of the stress vector at $x_1=\pm s/2$

$$R_0-2c\alpha=\mu\sqrt{3}(\bar{\gamma}+C) \tag{27}$$

The wanted constants are deduced from the previous equations:

$$C=\frac{R_0-\sqrt{3}\mu\bar{\gamma}}{\sqrt{3}\mu+\frac{12cl}{\sqrt{3}s^3}},\quad D=-C\frac{l}{2},\quad \alpha=-\frac{12}{\sqrt{3}}\frac{D}{s^3} \tag{28}$$

The obtained profiles of plastic strain and displacement are illustrated in Figure 2 for the material parameters listed in Table 1. These parameters correspond typically to a bimetal laminate with a yield stress $R_0=20$ MPa in the soft phase and an intrinsic length $l_c=\sqrt{c/\mu}=0.4\,\mu$m, leading to strong size effects in the micron range and below.

The macroscopic stress is equal to the uniform value σ_{12}. It can be related to the macroscopic applied shear as

$$\frac{\sigma_{12}}{\mu}=\frac{R_0}{\sqrt{3}\mu+\frac{12cl}{\sqrt{3}s^3}}+\bar{\gamma}\frac{4cl}{\mu s^3+4cl}=\frac{1}{\mu fs^2+4c}\left(\frac{\sqrt{3}}{3}fs^2R_0+4c\bar{\gamma}\right) \tag{29}$$

Two limit cases arise naturally. For a constant volume fraction f, an increasing size $s\to\infty$ leads to the classic size-independent yield stress $\sigma_{12}=R_0/\sqrt{3}$. When s becomes vanishingly small, a purely elastic law is retrieved: $\sigma_{12}=\mu\bar{\gamma}$.

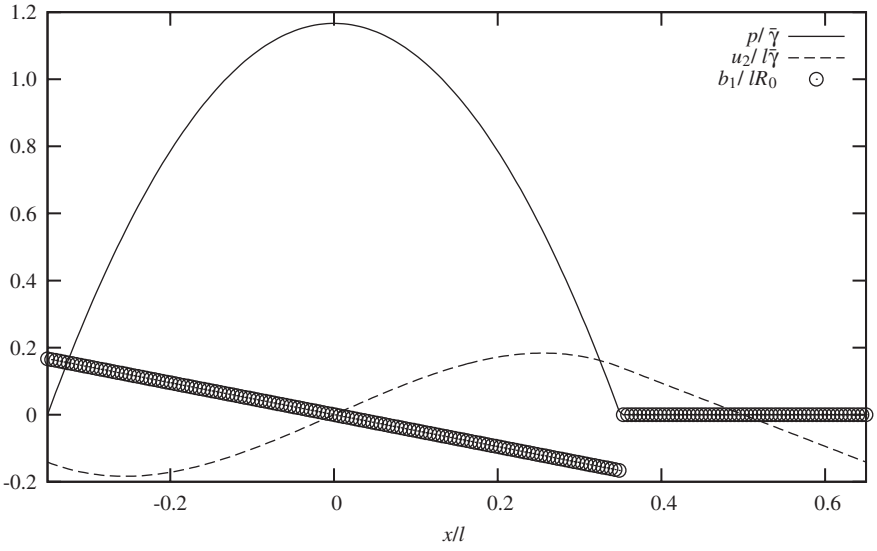

Figure 2 Normalized profiles of plastic strain, vertical displacement, and horizontal double traction component in a shear unit cell of size l according to strain gradient plasticity.

Table 1 Material and geometric parameters of a laminate microstructure made of strain gradient plasticity material.

μ (MPa)	R_0 (MPa)	c (MPa mm^2)	f	l (μm)	$\bar{\gamma}$
30,000	20	0.005	0.7	10	0.01

It should be noted that the previous solution implies a jump of the higher-order stress $b_1=2c\alpha$ at the interface $s=\pm s/2$:

$$b_1\left(\frac{s^+}{2}\right)-b_1\left(\frac{s^-}{2}\right)=0-c\alpha s,\quad [\![b_1]\!]\left(\frac{s}{2}\right)=-c\alpha s \tag{30}$$

3.3 Scaling law

The plastic strain is

$$\varepsilon^p_{12}=\varepsilon_{12}-\varepsilon^e_{12}\quad\Rightarrow\quad \sqrt{3}p=\bar{\gamma}+u^s_{,1}-\frac{\sigma_{12}}{\mu} \tag{31}$$

The averaged plastic strain over the unit cell is

$$\bar{p}=\frac{1}{l}\int_{-s/2}^{s/2}p(x_1)dx_1\quad\Rightarrow\quad \sqrt{3}\bar{p}=f\bar{\gamma}+\frac{1}{l}\left(u^s\left(\frac{s}{2}\right)-u^s\left(-\frac{s}{2}\right)\right)-f\frac{\sigma_{12}}{\mu} \tag{32}$$

The relative displacement appearing in the last equation is found to be

$$u^s\left(\frac{s}{2}\right)-u^s\left(-\frac{s}{2}\right)=-Ch\quad\Rightarrow\quad \sqrt{3}\bar{p}=f\bar{\gamma}-C(1-f)-f\frac{\sigma_{12}}{\mu} \tag{33}$$

The combination of this expression of the plastic strain as a function of $\bar{\gamma}$ with (29) relating the stress to the applied shear provides the relation linking the current yield stress to overall plastic strain:

$$\sigma_{12}=\frac{R_0}{\sqrt{3}}+\frac{4\sqrt{3}cl}{s^3}\bar{p}=\frac{R_0}{\sqrt{3}}+\frac{4\sqrt{3}c}{f^3l^2}\bar{p} \tag{34}$$

This homogenized hardening law clearly shows the additional linear isotropic hardening induced by the intrinsic length associated with parameter c. For a vanishing c, the usual size-independent constant yield strength is retrieved. The relation (34) also reveals the scaling law between the size-dependent extrastress $\sigma_{12}-R_0/\sqrt{3}$ and the unit cell size l for a given volume fraction f.

4 Size effect in a laminate according to isotropic microplasticity

The previous boundary value problem is now reconsidered when the material is treated as a two-phase microplastic continuum with the following simple free energy density function:

$$\rho\psi(\underset{\sim}{\varepsilon}^e,p,p_\chi,\nabla p_\chi)=\frac{1}{2}\underset{\sim}{\varepsilon}^e:\underset{\approx}{\boldsymbol{C}}:\underset{\sim}{\varepsilon}^e+\frac{1}{2}H_\chi(p-p_\chi)^2+\frac{1}{2}A\nabla p_\chi\cdot\nabla p_\chi \tag{35}$$

In the elastic phase h, the variable $p=0$ and the material parameter A is called A^h. For the sake of brevity, the same value of H_χ is used for both phases.

The generalized stresses associated with the state variables are derived from partial derivation of the free energy potential:

$$\begin{aligned}&\underset{\sim}{\boldsymbol{\sigma}}=\rho\frac{\partial\psi}{\partial\underset{\sim}{\varepsilon}^e}=\underset{\approx}{\boldsymbol{C}}:\underset{\sim}{\varepsilon}^e,\quad R=\rho\frac{\partial\psi}{\partial p}=H_\chi(p-p_\chi),\\ &\underline{b}=\rho\frac{\partial\psi}{\partial\nabla p_\chi}=A\nabla p_\chi,\quad a=\rho\frac{\partial\psi}{\partial p_\chi}=-H_\chi(p-p_\chi)\end{aligned} \tag{36}$$

The additional balance equation for a and $\underline{\boldsymbol{b}}$ is

$$a=\operatorname{div}\underline{\boldsymbol{b}}\quad\Rightarrow\quad p_\chi-\frac{A}{H_\chi}p_{\chi,11}=p \tag{37}$$

4.1 Resolution for the laminate microstructure

The shear stress is uniform throughout the laminate and takes the value

$$\sqrt{3}\sigma_{12}=R_0+R=R_0+H_\chi(p-p_\chi)=R_0-Ap_{\chi,11} \tag{38}$$

Derivation of the previous equations with respect to x_1 shows that $p_{\chi,111}=0$, which leads to the following profile of the microplastic deformation in the soft phase:

$$p_\chi(x)=\alpha x^2+\beta,\quad \forall|x|\le\frac{s}{2} \tag{39}$$

where α and β are integration constants to be determined. It follows that

$$\sqrt{3}\sigma_{12}=R_0-2A\alpha \tag{40}$$

The plastic strain distribution follows:

$$p=\alpha x^2+\beta-\frac{2A}{H_\chi}\alpha, \quad \forall |x|\le\frac{s}{2} \tag{41}$$

In the hard elastic phase, the solution of (38) with $p=0$ yields

$$p_\chi^h=\alpha_h\cosh\omega_h\left(x-\frac{l}{2}\right), \quad \frac{s}{2}\le x\le\frac{s}{2}+h, \quad \text{with} \quad \omega_h^2=\frac{H_\chi}{A_h} \tag{42}$$

Two relations between the integration constants are first derived from two interface conditions:

– Continuity of microplastic deformation at $x=s/2$:

$$\alpha\frac{s^2}{4}+\beta=\alpha_h\cosh\omega_h\frac{h}{2} \tag{43}$$

– Continuity of the generalized stress component b_1:

$$A\alpha s=-A_h\alpha_h\omega_h\sinh\omega_h\frac{h}{2} \tag{44}$$

It is recalled that $\dot\varepsilon_{12}^p=\sqrt{3}\dot p/2$, so that the displacement in the plastic phase can be expressed as:

$$\begin{aligned} u^s_{,1}&=\frac{\sigma_{12}}{\mu}-\bar\gamma+\sqrt{3}p\\ &=\frac{1}{\mu\sqrt{3}}(R_0-2A\alpha)-\bar\gamma+\sqrt{3}\left(\alpha x^2+\beta-\frac{2A}{H_\chi}\alpha\right)\\ u^s&=\alpha\frac{x^3}{\sqrt{3}}+\left(\sqrt{3}\beta-\bar\gamma+\frac{R_0}{\sqrt{3}\mu}-2A\alpha\left(\frac{1}{\sqrt{3}\mu}+\frac{\sqrt{3}}{H_\chi}\right)\right)x \end{aligned} \tag{45}$$

where the integration constant has been chosen by setting $u(0)=0$.

The displacement in the elastic phase is obtained as

$$u^h=\left(\frac{1}{\sqrt{3}\mu}(R_0-2A\alpha)-\bar\gamma\right)x+C \tag{46}$$

where a new integration constant C arises.

Two additional relations between the integration constants are derived from requirements for the displacement field:

– Continuity of the displacement at $x=s/2$: $u^s(s/2)=u^h(s/2)$

$$\alpha\frac{s^3}{8\sqrt{3}\mu}+\sqrt{3}\left(\beta-\frac{2A\alpha}{H_\chi}\right)\frac{s}{2}=C \tag{47}$$

– Periodicity of the displacement component $u^s(-s/2)=u^h(s/2+h)$

$$-\left(\frac{\sigma_{12}}{\mu}-\bar\gamma\right)l+\sqrt{3}\left(\beta+\frac{2A\alpha}{H_\chi}\right)\frac{s}{2}-\alpha\frac{s^3}{8\sqrt{3}}=C \tag{48}$$

The combination of (47) and (48) leads to the following equation:

$$\alpha\left(\frac{s^3}{4\sqrt{3}}-2A\left(\frac{\sqrt{3}s}{H_\chi}+\frac{l}{\sqrt{3}\mu}\right)\right)+\sqrt{3}\beta s=\left(\bar\gamma-\frac{R_0}{\sqrt{3}\mu}\right)l \tag{49}$$

The combination of (43) and (44) leads to the following equation:

$$\alpha\left(\frac{s^2}{4}+\frac{A}{A^h}\frac{s}{\omega_h}\operatorname{cotanh}\omega_h\frac{h}{2}\right)+\beta=0 \tag{50}$$

The previous equations are necessary and sufficient for the determination of the constants α, β, α^h, and C. The fields of plastic strain, plastic microdeformation, and displacement follow. They are illustrated in Figure 3 for which the material and geometrical parameters of Table 1 are used. The parameter c of Table 1 is replaced by $A=A_h=0.005$ MPa mm^2 and $H_\chi=50{,}000$ MPa. Figure 3 shows that, for this high value of H_χ, the microplastic strain p_χ is very close to p. It is worth noting that, in contrast to p, p_χ does not vanish in phase h. In contrast to strain gradient plasticity, the double traction component does not vanish in phase h either. The double traction is continuous at the interface. However, the decrease of b_1 is very steep for x larger but close to $s/2$.

4.2 Scaling law

The scaling law results from the expression of the overall stress σ_{12} as a function of the mean plastic strain over the unit cell:

$$\begin{aligned} \bar p&=\frac{1}{l}\int_{-\frac{s}{2}}^{\frac{s}{2}}\left(\alpha x^2+\beta-\frac{2A\alpha}{H_\chi}\right)dx\\ &=f\left(\alpha\left(\frac{s^2}{12}-\frac{2A}{H_\chi}\right)+\beta\right)=\beta f\left(1-\frac{1}{L^2}\left(\frac{s^2}{12}-\frac{2A}{H_\chi}\right)\right) \end{aligned} \tag{51}$$

with $L^2=\frac{s^2}{4}+\frac{A}{A_h}\frac{s}{\omega_h}\operatorname{cotanh}\omega_h\frac{h}{2}=-\frac{\beta}{\alpha}$. The uniform stress component can now be expressed as a function of the volume fraction f of the soft phase and of the unit cell size l:

$$\sqrt{3}\sigma_{12}=R_0+\frac{2A}{f}\frac{\bar p}{\frac{f^2l^2}{6}+\frac{2A}{H_\chi}+\frac{A}{A_h}\frac{fl}{\omega_h}\operatorname{cotanh}\omega_h\frac{h}{2}} \tag{52}$$

This homogenized relation reveals the macroscopic linear hardening that results from the micromorphic

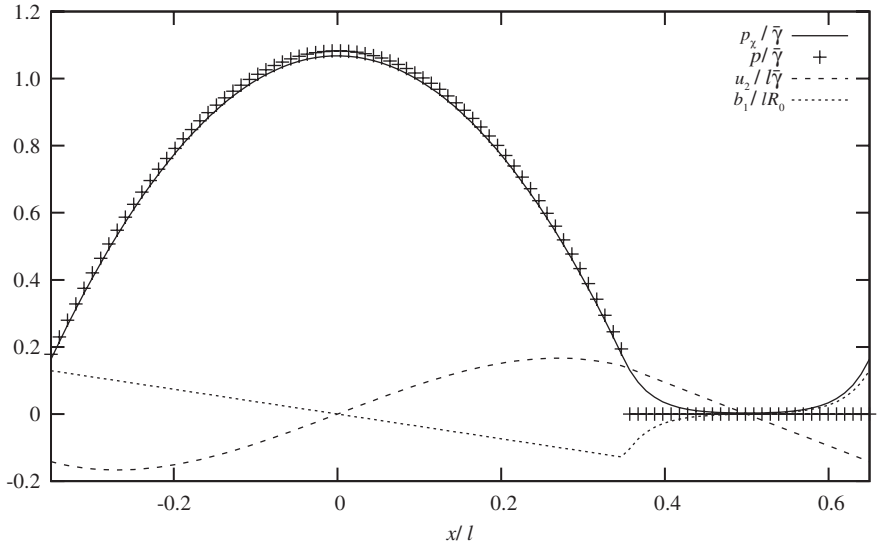

Figure 3 Normalized profiles of plastic strain, vertical displacement, and horizontal double traction component in a sheared unit cell of size l according to micromorphic plasticity.

effects taking place inside the microstructure. The found scaling of the effective hardening modulus is the same as for strain gradient plasticity, namely, l^2.

A first limit case of interest is obtained for $H_\chi \to \infty$ for which the strain gradient plasticity model is retrieved in the form of (34) as the limit of (52).

A second important limit case is found for the unit cell size l tending to zero:

$$\sqrt{3}\sigma_{12} - R_0 \sim H_\chi \frac{1-f}{f}\bar{p} \tag{53}$$

This proves that the microplastic deformation model leads to a saturation of the size-dependent hardening effect, which is in contrast to the asymptotic behavior of Aifantis model, see (34). This saturation is visible on the log-log diagram of Figure 4.

For a fixed offset macroscopic plastic strain $\bar{p}$, the overall yield stress given by (53) tends to infinity when the parameter $H_\chi \to \infty$, thus retrieving the unbounded response of Aifantis strain gradient model.

5 Discussion

It is noteworthy that the previous simple strain gradient plasticity models that involve only one or two additional material parameters compared with the original classic J_2 plasticity model give rise to clear size effects regarding the plasticity distribution in the soft phase, on the one hand, and the overall hardening behavior, on the other hand.

The parabolic distribution of plastic strain inside the channel of soft phase is reminiscent of the dislocation gliding mechanism through the channel and the piling up of dislocations along the channel walls. It corresponds to the exact solution of the line tension dislocation model, as shown in [26]. Such nonhomogeneous distributions of plastic slip were also observed in a sheared layer in dislocation dynamics simulations as well as strain gradient plasticity simulations [27, 28]. More general *cosh* profiles are obtained in the presence of classic isotropic hardening in the plastic phase [24]. These profiles were also discussed in [25, 29], but corresponding scaling laws were note explicitly provided.

The Aifantis and micromorphic models give rise to an overall linear hardening directly related to the plastic layer thickness and the additional material parameters. Let us recall the obtained effective hardening modulus, called $\bar{H}$ for Aifantis model and $\bar{H}_\chi$ for the micromorphic model:

$$\bar{H} = \frac{4\sqrt{3}c}{f^3 l^2}, \quad \bar{H}_\chi = \frac{1}{\sqrt{3}f}\frac{2A}{\dfrac{f^2 l^2}{6} + \dfrac{2A}{H_\chi} + \dfrac{A}{A_h}\dfrac{fl}{\omega_h}\operatorname{cotanh}\omega_h \dfrac{h}{2}} \tag{54}$$

They respectively come from (34) and (52) of the previous sections. They involve one (two) constitutive parameter for the strain gradient (micromorphic) model and the unit cell thickness l and volume fraction f of the plastic

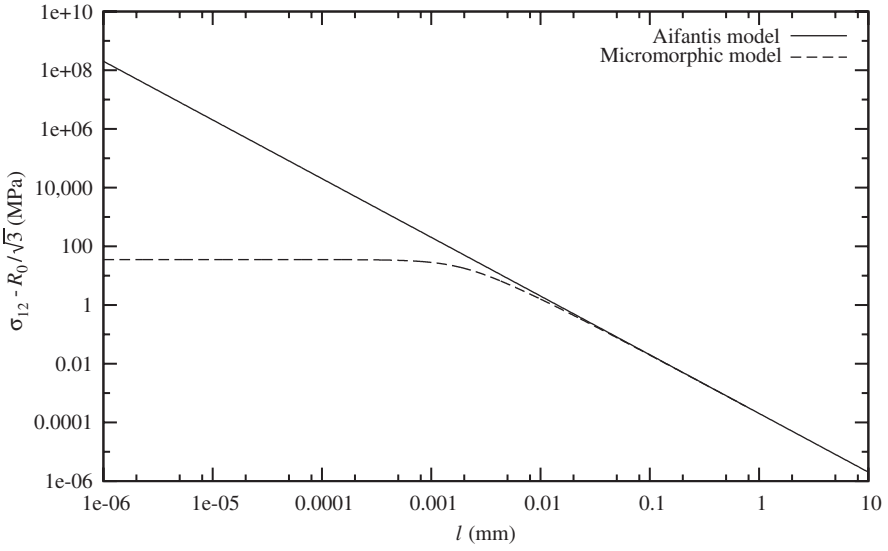

Figure 4 Overall yield stress at 0.2% average plastic strain for a laminate microstructure as a function of the unit cell size l according to the micromorphic and the strain gradient plasticity models.

phase. Within the isotropic Aifantis model, this linear hardening is of isotropic nature. Such a linear or quasi-linear hardening also exists for single crystals undergoing single or multiple slip [30, 31], but it is of intrinsic kinematic nature, thus representing a back-stress [23]. This is due to the fact that the state variable of gradient crystal plasticity is not the gradient of the cumulative plastic strain but rather the dislocation density tensor, defined as the curl of the plastic deformation.

A remarkable feature of (54) is the inverse quadratic dependence of the effective modulus on l. The same l^2 scaling of the effective hardening modulus with the microstructure size has been found for a single crystal model involving single or double slip, based on the same micromorphic formulation [6, 24]. Aifantis model exhibits this scaling over the entire range of lengths l, whereas the micromorphic displays a saturation at tiny length scales with a transition from the l^2 regime to the saturation domain. The transition regime corresponds to a varying size dependence that can be adjusted from experimental data by identifying the suited parameter A and H_χ, see [6, 32].

Based on the overall behavior of the laminate, an overall yield stress at 0.2% can be defined that follows the same l^2 scaling as the effective hardening modulus. Nevertheless, it is apparent that the initial yield stress of the composite is the same as the one of the bulk soft phase. This is sometimes seen as a failure of the strain gradient plasticity model to address the initial Hall-Petch effect. However, in polycrystals, the microplasticity threshold for a given grain size may well be the same as that of the bulk single crystal. Due to the presence of grain boundaries, pileups may form very early and induce a strong back-stress inhibiting the initial sources and leading to a strong initial hardening hardly distinguishable from the linear regime at the macroscale and leading to a higher apparent yield stress. This effect has been analyzed for polycrystals in [32]. However, the strain gradient hardening effect appears to be too low under multislip conditions in comparison with experimental results, at least in the simulation conditions of [2, 32, 33]. This shortcoming may (partly) be attributed to the simplistic strain gradient constitutive equations like the linear higher-order constitutive relations (11).

The saturation behavior of the micromorphic model is reminiscent of the response of nanocrystalline metals that exhibit a saturation of the Hall-Petch effect at grain sizes of the order of 20–50 nm possibly followed by inverse grain size effect due to the activation of grain boundary sliding and rearrangement [34]. The material parameters of the micromorphic model can be identified so as to mimic this nanocrystalline behavior.

What is the relevance of a l^2 scaling of the yield stress or hardening modulus for a laminate from the point of view of physical metallurgy? The analysis of periodic pileups in a narrow channel in [35] rather leads to a l^1 scaling that seems to be consistent with experimental evidence of thin film or layer behavior. This analytical result therefore questions again the relevance of the constitutive equations and expresses a need for more elaborate

strain gradient behavior laws. The quadratic potential with respect to the plastic strain gradient that is necessary to obtain a Helmholtz type of balance equation (12) has been reconsidered in [36, 37]. These authors introduce the Euclidean norm of the dislocation density tensor instead of its square. This choice leads to strongly nonlinear constitutive and partial differential equations that require systematic further analysis. Also, the examples were given here in the case of gradient contributions arising solely from the stored energy function. More general splits of this contribution into stored and dissipative parts must now be investigated following [7, 22, 38].

References

[1] Mühlhaus HB. *Continuum Models for Materials with Microstructure*. Wiley: New York, 1995.
[2] Forest S, Barbe F, Cailletaud G. *Int. J. Solids Struct*. 2000, 37, 7105–7126.
[3] Cheong KS, Busso EP, Arsenlis A. *Int. J. Plast*. 2005, 21, 1797–1814.
[4] Bayley CJ, Brekelmans WAM, Geers MGD. *Philos. Mag*. 2007, 87, 1361–1378.
[5] Bargmann S, Ekh M, Runesson K, Svendsen B. *Philos. Mag*. 2010, 90, 1263–1288.
[6] Cordero NM, Gaubert A, Forest S, Busso E, Gallerneau F, Kruch S. *J. Mech. Phys. Solids* 2010, 58, 1963–1994.
[7] Forest S. *ASCE J. Eng. Mech*. 2009, 135, 117–131.
[8] Forest S, Aifantis EC. *Int. J. Solids Struct*. 2010, 47, 3367–3376.
[9] Mindlin RD. *Arch. Rat. Mech. Anal*. 1964, 16, 51–78.
[10] Eringen AC, Suhubi ES. *Int. J. Eng. Sci*. 1964, 2, 189–203, 389–404.
[11] Germain P. *SIAM J. Appl. Math*. 1973, 25, 556–575.
[12] Fleck NA, Hutchinson JW. *J. Mech. Phys. Solids* 2001, 49, 2245–2271.
[13] Engelen RAB, Geers MGD, Baaijens FPT. *Int. J. Plast*. 2003, 19, 403–433.
[14] Aifantis EC. *J. Eng. Mater. Technol*. 1984, 106, 326–330.
[15] Aifantis EC. *Int. J. Plast*. 1987, 3, 211–248.
[16] Forest S, Sievert R, Aifantis EC. *J. Mech. Behav. Mater*. 2002, 13, 219–232.
[17] de Borst R, Sluys LJ, Mühlhaus HB, Pamin J. *Eng. Comput*. 1993, 10, 99–121.
[18] de Borst R, Pamin J. *Int. J. Numer. Methods Eng*. 1996, 39, 2477–2505.
[19] de Borst R, Pamin J, Geers MGD. *Eur. J. Mech. A/Solids* 1999, 18, 939–962.
[20] Forest S, Sievert R. *Acta Mech*. 2003, 160, 71–111.
[21] Gurtin ME. *Int. J. Plast*. 2003, 19, 47–90.
[22] Gurtin ME, Anand L. *J. Mech. Phys. Solids* 2009, 57, 405–421.
[23] Forest S. *Philos. Mag*. 2008, 88, 3549–3563.
[24] Aslan O, Cordero NM, Gaubert A, Forest S. *Int. J. Eng. Sci*. 2011, 49, 1311–1325.
[25] Forest S, Bertram A. Formulations of strain gradient plasticity. In: *Mechanics of Generalized Continua*, Altenbach H, Maugin GA, Erofeev V, Eds. Advanced Structured Materials vol. 7. Springer: Berlin, Heidelberg, 2011, pp. 137–150.
[26] Forest S, Sedláček R. *Philos. Mag*. A 2003, 83, 245–276.
[27] Shu JY, Fleck NA, Van der Giessen E, Needleman A. *J. Mech. Phys. Solids* 2001, 49, 1361–1395.
[28] Bittencourt E, Needleman A, Gurtin ME, Van der Giessen E. *J. Mech. Phys. Solids* 2003, 51, 281–310.
[29] Cottura M, Le Bouar Y, Finel A, Appolaire B, Ammar K, Forest S. *J. Mech. Phys. Solids* 2012, 60, 1243–1256.
[30] Bayley CJ, Brekelmans WAM, Geers MGD. *Int. J. Solids Struct*. 2006, 43, 7268–7286.
[31] Ertürk I, van Dommelen JAW, Geers MGD. *J. Mech. Phys. Solids* 2009, 57, 1801–1814.
[32] Cordero NM, Forest S, Busso EP. *Comptes Rendus Mécanique* 2012, 340, 261–274.
[33] Okumura D, Higashi Y, Sumida K, Ohno N. *Int. J. Plast*. 2007, 23, 1148–1166.
[34] Thomas O, Ponchet A, Forest S, Eds. *Mechanics of Nano-objects*. Presses des Mines, 2011, 380 pages. ISBN 978-2911256-67-7.
[35] Tanaka K, Mura T. *J. Appl. Mech*. 1981, 48, 97–103.
[36] Ohno N, Okumura D. *J. Mech. Phys. Solids* 2007, 55, 1879–1898.
[37] Conti S, Ortiz M. *Arch. Rat. Mech. Anal*. 2005, 176, 103–147.
[38] Anand L, Aslan O, Chester SA. *Int. J. Plast*. 2012, 30–31, 116–143.